CoMFA and Homology-Based Models of the Glycine Binding Site of *N*-Methyl-D-aspartate Receptor

Irina G. Tikhonova, Igor I. Baskin, Vladimir A. Palyulin, and Nikolai S. Zefirov*

Department of Chemistry, Moscow State University, Moscow 119992, Russia

Received August 2, 2002

Homology modeling was used to build 3D models of the *N*-methyl-D-aspartate (NMDA) receptor glycine binding site on the basis of an X-ray structure of the water-soluble AMPA-sensitive receptor. The docking of agonists and antagonists to these models was used to reveal binding modes of ligands and to explain known structure−activity relationships. Two types of quantitative models, 3D-QSAR/CoMFA and a regression model based on docking energies, were built for antagonists (derivatives of 4-hydroxy-2-quinolone, quinoxaline-2,3-dione, and related compounds). The CoMFA steric and electrostatic maps were superimposed on the homology-based model, and a close correspondence was marked. The derived computational models have permitted the evaluation of the structural features crucial for high glycine binding site affinity and are important for the design of new ligands.

Introduction

The activation of postsynaptic *N*-methyl-D-aspartate (NMDA) receptor channels by the native agonist glutamate and coagonist glycine (or D-serine[1]) leads to calcium influx into the neuron, and this process plays a key role in memory formation and neurotoxicity.[2,3] Therefore, it is generally agreed that NMDA receptor malfunctioning is involved in many neurodegenerative disorders.

Several potential loci can been distinguished for modulation of NMDA receptor activity, including the glutamate and glycine agonist binding sites,[4] the polyamine modulator sites (voltage-dependent and voltage-independent, respectively), and sites associated with the ion channel.[5] The discovery that antagonists of the glycine site may lack certain undesirable side effects observed for many noncompetitive and competitive antagonists has increased interest in this target. Many publications deal with the synthesis and structure−activity relationships of glycine site antagonists[6−13] belonging to seven main classes: kynurenic acid derivatives, 2-carboxyindoles, 2-carboxytetrahydroquinolines, 4-hydroxy-2-quinolones, quinoxaline-2,3-diones, 6-hydroxy-1*H*-1-benzazepine-2,5-diones, and tricyclic compounds.

Some attempts to rationalize known structure−activity relationships have been made. Sui Xlong Cal and colleagues proposed a scheme of hydrogen-bonding and charge−charge interactions of 1,2,3,4-tetrahydroquinoline-2,3,4-trione 3-oxime and quinoxaline-2,3-dione antagonists in the glycine site on the basis of the affinity measurements.[7] Other authors suggested a pharmacophore model of the glycine site for the cases of indole-2-carboxylates,[8] kynurenic acid derivatives,[9] and 4-amino-2-carboxytetrahydroquinolines.[10] In 1997, a first 3D model of the glycine site was built on the basis of amino acid sequence homology (∼18%) with the bacterial periplasmic protein LAOBP for the open form of the protein domain, and the binding modes of agonists and antagonists were suggested.[14]

In this study, we have built[4c] and refined with molecular mechanics optimization and molecular dynamics simulations homology-based (∼29%) models of the glycine site using recently reported X-ray crystallographic analyses of a water-soluble AMPA-sensitive glutamate receptor and its complexes with different ligands[15] for the antagonist-binding open and agonist-binding closed forms of the glycine site. With these models, we have performed docking of agonists and antagonists as a way of exploring their binding modes and explaining known structure−activity relationships and previously reported pharmacophore models. For the most studied classes of antagonists, derivatives of 4-hydroxy-2-quinolone, quinoxaline-2,3-dione, and related compounds, we have built two quantitative structure−activity models, one of which was ligand-based (using the CoMFA methodology[16]) while the other was based on docking energies. In addition, we have superimposed CoMFA maps with protein models and demonstrated their compatibility. All these approaches produced a consistent model of ligand−protein interactions, which can further be used for designing new NMDA receptor glycine site ligands.

Methods

For modeling the glycine site of the NMDA receptor, a multiple alignment was built for the primary sequences of all representatives of the ionotropic glutamate receptors family, namely, NR1 (Swiss protein data bank[17] accession code P35437), NR2A (Q12879), NR2B (Q13224), NR2C (Q14957), NR2D (Q15399), GLUR1 (P42261), GLUR2 (P42262), GLUR3 (P42263), GLUR4 (P48058), GLUR5 (P39086), GLUR6 (Q13002), KA1 (Q16099), and KA2 (Q16478) subunits and the sequence of the genetically constructed water-soluble AMPA-sensitive glutamate receptor[15] (AMPASGR) by means of the Clustal X program.[18] The BLOSUM30 homology matrix was used for evaluating amino acid similarity. The homology modeling was performed using the Biopolymer module of the Sybyl 6.6 molecular modeling package on an SGI Octane workstation.[19] The X-ray structures of the AMPASGR complexed with glutamate, the native agonist of all glutamate

* To whom correspondence should be addressed. Phone: +7-095-9393557. Fax: +7-095-9390290. E-mail: zefirov@org.chem.msu.su.

10.1021/jm0210156 CCC: $25.00
Published on Web 03/29/2003

Table 1. Antagonists Included in CoMFA and Docking Studies

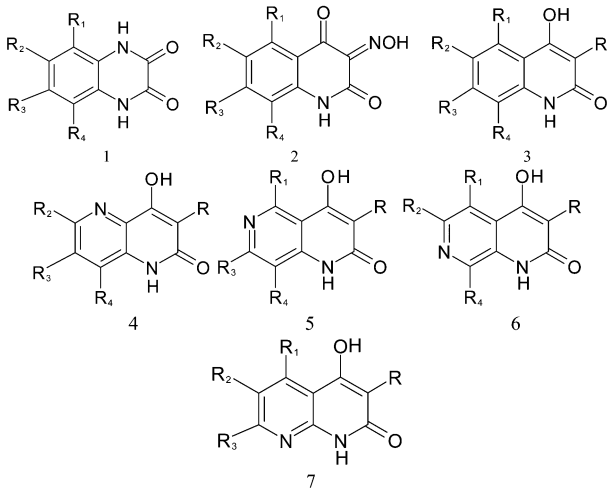

compd	R	R_1	R_2	R_3	R_4	St[a]	IC_{50}([^{3}H]DCKA) (μM)	$\log(1/IC_{50})$	E_{el} (kcal/mol)	E_{st} (kcal/mol)	ref
1		NO_2	Cl	Cl	H	1	0.0059 ± 0.001	2.23	−19.85	−91.96	11
2		H	Me	Me	H	1	3.3 ± 0.7	−0.52	−11.32	−6.24	11
3		H	Cl	Et	H	1	1.4 ± 0.2	−0.15	−9.85	−5.63	11
4		H	Et	Et	H	1	1.8 ± 0.2	−0.26	−12.38	−61.36	11
5		H	OMe	OMe	H	1	17 ± 1	−1.23	−6.67	−58.13	11
6		H	OCH_2O		H	1	>100	−2.00	−8.27	−20.79	11
7		H	CH=CHCH=CH		H	1	16 ± 1	−1.20	−4.24	65.45	11
8		H	$CH_2CH_2CH_2$		H	1	15 ± 4	−1.17	−4.43	−63.18	11
9		NO_2	H	Me	H	1	9.3 ± 1.9	−0.97	−8.29	−62.66	11
10		H	OMe	Br	H	1	1.0 ± 0.2	0	−11.61	−71.84	11
11		H	OH	OH	H	1	>100	−2.00	−9.44	−49.56	11
12		H	Cl	Me	H	1	0.78 ± 0.06	−0.11	−4.55	−61.58	11
13		NO_2	Me	Me	H	1	0.029 ± 0.003	1.54	−14.32	−72.56	11
14		NO_2	Et	Et	H	1	0.16 ± 0.03	0.80	−8.95	−65.06	11
15		NO_2	$CH_2CH_2CH_2$		H	1	3.1 ± 0.5	−0.49	−0.33	−25.02	11
16		NO_2	OMe	Br	H	1	0.064 ± 0.003	1.19	−11.36	−78.54	11
17		NO_2	Br	Et	H	1	0.082 ± 0.019	1.09	−15.85	−62.69	11
18		NO_2	Cl	Et	H	1	0.029 ± 0.002	1.54	−10.90	−84.51	11
19		NO_2	Et	Cl	H	1	0.13 ± 0.01	0.89	−11.30	−51.68	11
20		NO_2	Me	CN	H	1	0.073 ± 0.01	1.14	−9.05	−61.66	11
21		NO_2	Me	F	H	1	0.095 ± 0.024	1.02	−8.21	−62.04	11
22		NO_2	Me	Br	H	1	0.0087 ± 0.0004	2.06	−18.48	−89.09	11
23		NO_2	Me	Cl	H	1	0.0047 ± 0.0006	2.33	−19.68	−84.30	11
24		NO_2	Cl	Me	H	1	0.045 ± 0.008	1.35	−16.52	−85.83	11
25		NO_2	H	CN	H	1	2.8 ± 0.4	−0.45	−6.00	−35.29	11
26		NH_2	Me	Cl	H	1	0.15 ± 0.03	0.82	−14.40	−46.10	11
27		NO_2	NH_2	F	H	1	11 ± 1	−1.04	−7.99	−41.51	11
28		NO_2	OMe	F	H	1	1.9 ± 0.1	−0.28	−8.71	−32.20	11
29		NO_2	SEt	Cl	H	1	0.64 ± 0.13	0.19	5.62	−42.75	11
30		NO_2	OEt	F	H	1	3.6 ± 0.7	−0.56	−9.80	−30.78	11
31		NO_2	OBu-n	F	H	1	4.3 ± 0.5	−0.63	−13.86	−30.40	11
32		NO_2	$O(CH_2)_3Ph$	F	H	1	4.0 ± 0.9	−0.60	−16.58	−87.13	11
33		NO_2	OMe	Cl	H	1	0.15 ± 0.02	0.82	−9.19	−78.34	11
34		OCOMe	OMe	OMe	H	1	53 ± 16	−1.72	−6.41	−40.32	11
35		OH	OMe	OMe	H	1	17 ± 2	−1.23	−7.24	−32.78	11
36		H	Cl	Cl	H	1	0.13 ± 0.03	0.89	−13.80	−72.31	11
37		H	H	H	H	1	9.8 ± 0.6	−0.99	−7.72	−39.86	7
38		H	H	Cl	H	1	1.8 ± 0.3	−0.25	−9.24	−46.89	7
39		Cl	H	Cl	H	1	0.28 ± 0.02	0.55	−9.82	−61.00	7
40		H	Cl	Cl	H	1	0.13 ± 0.03	0.89	−7.63	−54.60	7
41		Cl	Cl	Cl	H	1	0.03 ± 0.005	1.53	−8.44	−68.76	7
42		Me	H	Me	H	1	2.1 ± 0.1	−0.32	−4.51	−32.23	7
43		H	F	Cl	F	1	0.63 ± 0.11	0.20	−3.59	−57.85	7
44		F	F	F	F	1	0.73 ± 0.05	0.14	−9.06	−58.19	7
45		H	H	Cl	H	2	0.053 ± 0.003	1.28	−9.97	−30.05	7
46		H	H	H	Cl	2	>100	−2.00	−10.40	1.13	7
47		H	H	H	H	2	1.4 ± 0.2	−0.15	−13.37	−65.77	7
48		H	Cl	H	H	2	3.4 ± 0.3	−0.53	−9.97	−22.72	7
49		Cl	H	H	H	2	4.4 ± 0.4	−0.64	−7.49	−30.16	7
50		Cl	Cl	H	H	2	0.17 ± 0.03	0.77	−9.24	−46.90	7
51		Cl	H	Cl	H	2	0.033 ± 0.009	1.48	−12.29	−67.68	7
52		H	Cl	Cl	H	2	0.012 ± 0.001	1.92	−10.57	−87.13	7
53		Cl	Cl	Cl	H	2	0.007 ± 0.001	2.15	−17.95	−98.30	7
54		Me	H	Me	H	2	0.037 ± 0.004	1.43	−15.77	−67.37	7

Table 1 (Continued)

compd	R	R_1	R_2	R_3	R_4	St[a]	IC_{50}([^{3}H]DCKA) (μM)	$\log(^1/_{IC_{50}})$	E_{el} (kcal/mol)	E_{st} (kcal/mol)	ref
55		F	F	F	F	2	3.3 ± 0.7	−0.52	−4.00	−34.08	7
56		H	F	Cl	F	2	0.91 ± 0.08	0.04	−8.60	−51.50	7
57	NO_2	H	H	H	H	3	34 ± 3	−1.53	−3.79	−12.49	12
58	NO_2	H	H	Cl	H	3	1.5 ± 0.1	−0.18	−2.69	−12.28	12
59	NO_2	H	Cl	H	H	3	>100	−2.00	−0.10	−13.98	12
60	NO_2	Cl	H	H	H	3	61 ± 2	−1.78	−0.83	−12.90	12
61	NO_2	Cl	H	Cl	H	3	0.22 ± 0.05	0.66	2.32	−64.71	12
62	NO_2	H	Cl	Cl	H	3	0.4 ± 0.02	0.40	−1.06	−53.81	12
63	NO_2	Me	H	Me	H	3	0.29 ± 0.03	−0.54	−8.91	−9.16	12
64	NO_2	Cl	Cl	Cl	H	3	0.22 ± 0.04	0.66	3.13	−64.25	12
65	NO_2	H	H	H	Cl	3	>100	−2.00	10.28	−11.17	12
66	NO_2	H	Cl	Cl	Cl	3	>100	−2.00	−0.74	−7.17	12
67	NO_2	H	F	Cl	F	3	40 ± 5	−1.60	−7.91	−5.09	12
68	NO_2	F	F	F	F	3	>100	−2.00	−0.27	−6.26	12
69	*m*-$PhOC_6H_4$	H	H	Cl	H	4	0.023 ± 0.001	1.64	− 19.56	− 81.53	13
70	C_6H_5		H	H	H	4	>100	−2.00	−5.87	−12.16	13
71	C_6H_5		H	Cl	H	4	3.3 ± 0.7	−0.52	−6.28	−10.96	13
72	*p*-ClC_6H_4		H	Cl	H	4	13 ± 3	−1.11	−6.82	−10.79	13
73	*m*-ClC_6H_4		H	Cl	H	4	3.0 ± 0.1	−0.48	−11.09	−12.95	13
74	*o*-ClC_6H_4		H	Cl	H	4	24 ± 6	−1.38	0.96	−10.98	13
75	*m*-$MeOC_6H_4$		H	Cl	H	4	2.9 ± 0.2	−0.46	−0.57	−13.08	13
76	*m*-MeC_6H_4		H	Cl	H	4	1.8 ± 0.3	−0.25	−9.60	−8.06	13
77	*m*-$NO_2C_6H_4$		H	Cl	H	4	7.4 ± 1.6	−0.87	−8.22	−8.25	13
78	*m*-$PhOC_6H_4$		H	Cl	H	4	0.11 ± 0.02	0.96	−19.24	−34.16	13
79	3thienyl		H	Cl	H	4	4.3 ± 0.6	−0.63	−7.84	5.00	13
80	2thienyl		H	Cl	H	4	9.8 ± 1.9	−0.99	−13.23	−1.71	13
81	*m*-$PhOC_6H_4$	H		H	H	5	20 ± 5	−1.30	−2.1	−13.60	13
82	*m*-$PhOC_6H_4$	H	H		H	6	5.4 ± 1.3	−0.73	−3.19	−11.03	13
83	*m*-$PhOC_6H_4$	H	H	H		7	31 ± 7	−1.49	−7.90	−17.41	13
84	*m*-$PhOC_6H_4$	H	Cl	H		7	19 ± 3	−1.28	−7.26	3.71	13
85	C_6H_5	H	Cl	H		7	>100	−2.00	−1.67	−1.21	13
86	C_6H_5	H	H	H		7	>100	−2.00	10.27	−11.17	13
87	NO_2	H	H	Cl	H	7	1.5 ± 0.1	−0.18	−9.93	−3.06	13
88	NO_2		H	Cl	H	7	29 ± 4	−1.46	−9.66	−3.64	13

[a] St is the number of the templates.

receptors (1FTJ), and 6,7-dinitro-2,3-quinoxalinedione (DNQX), antagonist (1FTL) were used as templates for modeling the closed and open forms of the glycine binding site of the NMDA receptor.

In the course of molecular modeling, a template protein was mutated to the corresponding target protein in accordance with the procedure described elsewhere.[4] All insertions and deletions were handled by defining "loops" containing all residues being inserted and several neighboring atoms to the positions of insertion or deletion, followed by searching a database of protein loops for a proper template to model them. To remove distortions in geometry, the obtained protein was subjected to energy minimization using the Tripos force field as implemented in the Sybyl 6.6 package. Each protein model was then solvated with a box of water molecules and reminimized with the AMBER 6.0[20] program SANDER using the Cornell et al. force field.[21] This was followed by 150 ps of molecular dynamics simulation at 300 K using the same SANDER program.

The 3D profiles of models were tested with Verify3D,[22] while the stereochemical quality was checked using PROCHECK.[23,24]

Docking. A putative binding pocket was determined on the basis of data concerning site-directed mutagenesis.[14] Each ligand was placed into the binding pocket and orientated by taking into account the X-ray structures of AMPASGR−ligand complexes. A manual docking procedure was applied, and the obtained receptor−ligand complexes were optimized using the Tripos force field. Different conformations and orientations of each ligand within the binding pocket were explored, and each time the ligand−protein complex was reminimized. For clarifying the involvement of water molecules in ligand binding and for validating the docking modes, a 150 ps molecular dynamics simulation was carried out using SANDER with IBELLY restraints. Ab initio RESP[25] charges calculated with the 6-31G* basis set were assigned to ligand atoms. The energy decomposition analysis of interactions between ligands and amino acid residues forming the binding site was performed using the "anal" module of AMBER 6.0.

Preparation of Ligands for CoMFA Analysis. The models of all ligands were prepared using the Sybyl 6.6 molecular modeling software. All molecules were assumed to be protonated under physiological conditions. Their geometry was optimized using the Tripos force field (partial atomic charges were calculated using the Gasteiger−Hückel method). Low-energy conformations were found by systematic and grid conformational searches. For the CoMFA analysis, derivatives of 4-hydroxy-2-quinolone, quinoxaline-2,3-dione, and related compounds were aligned using the common 2-quinolone substructure as a template.

CoMFA Study. In the present study, the standard Sybyl 6.6 settings for the CoMFA procedure were applied. The CoMFA grid was extended beyond the superimposed molecules by at least 4 Å in all directions of the Cartesian coordinate system. An sp^3 carbon with a charge of +1 served as a probe atom. The CoMFA QSAR equations were derived with the partial least squares (PLS) method. The optimal number of components was selected as providing the highest cross-validation q^2 value. The $\log(^1/_{IC_{50}})$ values for inhibition of [3H]-DCKA binding[7,11−13] were used for expressing biological activity (Table 1).

Results and Discussion

Molecular Model of the NMDA Receptor Glycine Site and Docking of Some Ligands. Three-dimensional models of the glycine site of the NMDA receptor were built in two conformational states (closed, open) on the basis of sequence homology (∼29%) with AMPASGR. A putative binding site was located by taking into account positions of ligands in AMPASGR and results of site-directed mutagenesis experiments.[14] The energy-minimized structures of agonists (glycine, D-serine, D-cycloserine) and antagonists (derivatives of 4-hydroxy-2-quinolone, quinoxaline-2,3-dione, and re-

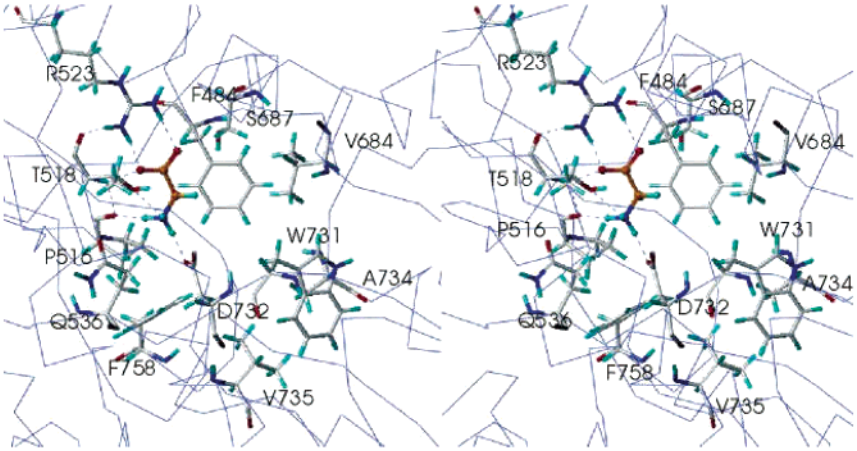

Figure 1. Binding mode of coagonist glycine to the NMDA receptor glycine binding site.

lated compounds (Table 1)) were manually docked into the binding site, while the closed and open forms of the receptor were used for docking agonists and antagonists, respectively. Molecular dynamics simulation of ligand−protein complexes revealed that the carboxyl group of agonists can form a salt bridge with R523 and hydrogen bonds with the NH group of T518 and the OH group of S687, while the amino group of glycine is predicted to bind to the carboxyl group of D732, carbonyl group of P516, and the hydroxyl group of T518 (Figure 1).

The binding energy contributions of amino acid residues forming the binding site are presented in Table 2. As can be seen, the main contribution for agonist binding is provided by R523 and D732. These residues lie in two different parts of the protein globule, and the interaction of agonists with them could be important for the globule collapse. This suggests that the main structural feature of an agonist should be the presence of one positively charged and one negatively charged center. This also explains the fact that carboxyl and amino termini must not be substituted for strong agonist activity (in fact, D-cycloserine has low agonist activity). It should be mentioned that direct involvement of R523 in agonist binding is supported by site-directed mutagenesis experiments,[14] while the influence of the D732A mutation on the agonist-induced receptor activity has been reported to be considerably weaker.[14]

To account for this supposed contradiction between the molecular model and the reduced influence of the D732A mutation on activity, we have performed the molecular dynamics simulation of the complex formed by the mutant protein with glycine. The binding energy contributions for this complex are given in Table 2. As can be seen from the comparison of the columns corresponding to the native and the mutant proteins in Table 2, the energy contributions have changed for several amino acids. While the interaction energy between the ligand and the amino acid in position 732 has almost vanished, this energy loss was partially compensated by the increase in interaction energies with T518, Q536, P516, and S688. These data, along with visual inspection, indicate that (1) the ligand has slightly changed its position in the binding site to accommodate this mutation and (2) the conformation of the side chain of Q536 has changed, so the amide group of this residue started to play a part of the carboxyl group in D732. This might account for the reduced influence of the D732A mutation on activity.

The docking and the molecular dynamics simulation of antagonists have revealed that they are anchored in the binding site mainly via a Coulombic interaction with R523, a hydrogen bond with T518, and a π-electron interaction with the aromatic ring of F484, in full agreement with previously reported pharmacophore models of NMDA receptor glycine site antagonists (a negatively charged part of a molecule and aromatic ring).[10] Their contributions to the binding energy are significant (see Table 2), and the importance of these residues is also supported by site-directed mutagenesis.[14] Although D732 does not interact with antagonists directly, the energy contribution of this residue is considerable (see Table 2) and it could be explained by the existence of long-range electrostatic interaction with antagonists. The details of ligand binding and substituent effects can be shown for the case of compound **23** (Figure 2 and Table 2). The hydrogen atoms in the 1- and 4-positions are H-bonded with P516 (1-position) and Q686 (4-position), the nitro group interacts with Q405 through a water molecule, the methyl group in the 6-position provides hydrophobic interactions with W731 and V735, and the chlorine atom in the 7-position lies in the hydrophobic pocket formed by F408 and A734.

This information can be compared with experimental results accumulated on structure−activity relationships for substituents.[7,11] For instance, close examination of molecular models reveals that (1) the 6-position should be occupied only by small hydrophobic substituents (e.g., $-CH_3$, $-Cl$) for increasing affinity because of a close distance between the ligand and W731, (2) the 7-position can accommodate bulk hydrophobic substituents, such as $-C_2H_5$, $-I$, and $-Br$, since it interacts with the hydrophobic pocket composed of F408 and A734, (3) the 8-position should not be substituted because of close contact to P516 and F758. This corresponds closely to experimental results.[11] Other experimental results that can be explained with these models deal with selectivity of quinoxaline-2,3-diones between NMDA and AMPA receptors. The superposition of glycine site antagonist complexes with the X-ray structure of the AMPASGR−DNQX complex indicates that the locations of A714 (not shown in Figure 2) and W731 in the glycine site near the 6-position of DNQX corresponds to S686 in AM-

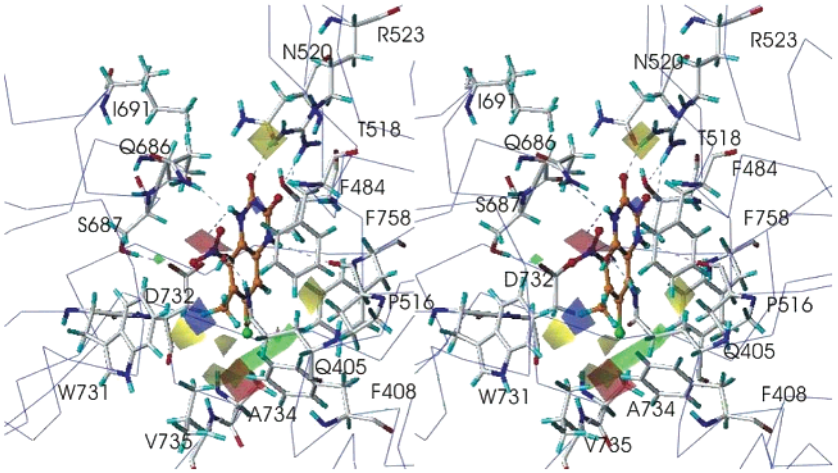

Figure 2. Binding mode of 7-chloro-6-methyl-5-nitro-1,4-dihydroquinoxaline-2,3-dione to the NMDA receptor glycine binding site. The superimposition of the CoMFA electrostatic and steric plots with the structural model of the binding site is shown. The sterically favored regions are shown in green, and the sterically disfavored regions are shown in yellow. The positive electrostatic contours are shown in blue, and negative electrostatic contours are shown in red.

Table 2. Binding Energy Contributions of Amino Acid Residues (in kcal/mol)

	ligand				
amino acid residue	glycine	glycine[a]	D-serine	D-cycloserine	compound **23**[b]
R523	−33.46	−28.696	−36.756	−15.455	−15.901
S687	−12.329	−12.751	−2.428	−4.277	−0.939
S688	−3.325	−4.146	−4.506	−4.545	−0.524
T518	−5.263	−15.404	−4.207	−7.616	−4.42
D732	−31.849		−32.728	−1.476	−12.656
A732		0.302			
P516	−8.995	−12.43	−10.944	−4.824	−5.411
V689	−0.015	−0.45	0.35	0.092	−0.06
F738	0	0	0	0	0
V684	−0.011	0.166	0.255	−0.897	−0.787
L538	−0.004	−0.018	0.054	−0.034	−0.065
W731	1.297	0.151	0.674	−0.182	−2.979
Q405	0.219	0	−7.404	−0.098	−0.958
F408	0.056	0.048	0.099	−0.053	−0.919
V735	0.055	0.095	0.102	−0.103	−0.616
F484	−2.063	−0.081	−2.771	−1.807	−10.781
F758	0.428	−0.218	0.044	−0.106	0.036
A734	−0.171	0.226	0.147	−0.307	0.007
Q536	0.01	−11.746	0.275	−0.056	−2.407
Q687	0	0	0	0	−4.057

[a] Binding of glycine with the mutant D732A. [b] Compound **23** is 7-chloro-6-methyl-5-nitro-1,4-dihydroquinoxaline-2,3-dione.

PASGR. Therefore, the presence of a hydrogen bond acceptor at the 6-position could increase the binding energy of quinoxaline-2,3-diones with the AMPA receptor. Indeed, the addition of a hydrogen bond acceptor, such as nitro, cyano, sulfamido, and imidazolyl groups, to the 6-position imparts potent AMPA antagonist activity,[27−31] whereas hydrophobic groups and halogens in this position are important for binding to the NMDA receptor glycine site.[31]

Pharmacophore of the Glycine Binding Site Antagonists. Several pharmacophore models for different classes of the glycine site antagonists have been discussed in the literature.[5−8] For the case of 2-quinolones, they include the presence of (1) H-bond acceptor in the 1-position, (2) a Coulombic interaction of substituent in position 2 with the binding site, (3) a bulk tolerance region at the 3-position, (4) the electropositive H-bonding region at the 4-position, (5) size-limited hydrophobic regions at the 5-, 6-, and 7-positions, and (6) a bulk region at the 8-position. On the basis of a 3D molecular model of the biotarget, one can interpret these pharmacophore regions. As can be seen from Figure 3 for the case of 2-quinolones, feature 1 is attributed to P516, the electrostatic interaction region (feature 2) is formed by R523 and T518, the bulk tolerance region (feature 3) is formed by interlobular space, the electropositive region (feature 4) is formed by the negatively charged Q405 and Q686 residues, the hydrophobic pocket (feature 5) is bordered by amino acids W731, A714, and V735, while the pocket (feature 6) is formed by P516 and F758.

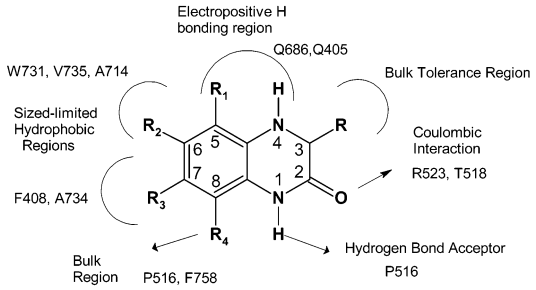

Figure 3. Pharmacophore model for NMDA receptor glycine binding site antagonists.

Quantitative Models. In addition to being used for qualitative analysis, molecular models of the glycine site can be useful for deriving and interpreting quantitative structure−activity relationships (QSARs). We have performed two kinds of QSAR studies for the glycine site antagonists. The first one was based on the CoMFA methodology,[12] while the second one utilized docking energies.

CoMFA Models. CoMFA models were developed using a training set of 88 derivatives of 4-hydroxy-2-quinolone, quinoxaline-2,3-dione, and related compounds (Table 1). Electrostatic and steric maps were used for describing molecular fields. The optimal number of components as determined by the PLS cross-validation procedure (the number of cross-validation groups was 10) appeared to be 5. For this case, the statistical parameters of the CoMFA model were the following: $q^2 = 0.801$; standard error of estimate was 0.376. The relative field contributions were 66.2% steric

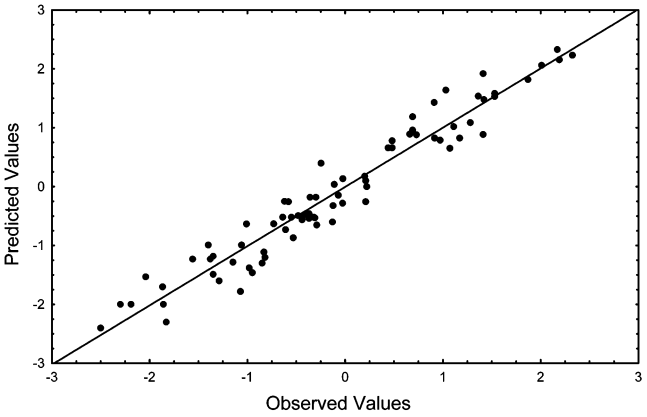

Figure 4. Correlation plot of observed vs predicted values of $\log(^1/_{IC_{50}})$ for the CoMFA model.

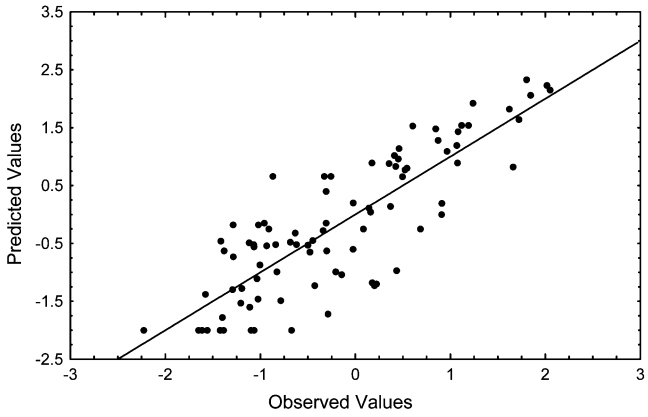

Figure 5. Correlation plot of observed vs predicted values of $\log(^1/_{IC_{50}})$ for the model based on docking energy.

and 33.8% electrostatic. The plot of actual vs calculated $\log(^1/_{IC_{50}})$ is presented in Figure 4.

Figure 2 illustrates the CoMFA electrostatic and steric maps superimposed on the structure of the most active compound in the training set. In this contour map, sterically favored regions are shown in green, sterically disfavored regions are shown in yellow, positive electrostatic contours are shown in blue, and negative electrostatic contours are shown in red. Structures from the training set allowed the receptor mapping in the neighborhood of positions 3, 4, 5, 6, 7, and 8 in 2-quinolones. The presence of a yellow color near the 8-position indicates the considerable decrease of activity upon introduction of any substituent into this position. The large green area around the 7-position indicates the presence of a pocket accommodating substituents of the appropriate size, including methyl, ethyl, etc., while the red area near this position indicates that such substituents could also be electronegative ones, such as halogens. A yellow area near the 6-position corresponds to the steric hindrance leading to the reduction of activity whenever the size of substituents at this position increases. Indeed, derivatives with 6-Cl and 6-Me show higher activity than compounds with larger groups carrying partial negative charge (e.g., methoxy). The preference for the methyl substituent over substituents carrying partial negative charges explains the presence of the blue area near this position. At the 4- and 5-positions, red and green areas indicate that electronegative groups are favored in these positions. The presence of a bulky substituent at the 3-position decreases activity because of steric hindrance, as indicated by the yellow contour.

The homology model of the glycine binding site can also be used for interpretation and validation of the CoMFA analysis results. The superimposition of the CoMFA electrostatic and steric plots with the model of the binding site in the open form (since it binds antagonists) shows a close correspondence (see Figure 2). The yellow color near 8-position corresponds to P516 and F758, the large green and red areas around the 7-position correspond to the hydrophobic pocket formed by A734 and F408, and the yellow and blue regions near the 6-position are attributed to W731. While the yellow region is a direct consequence of the bulkiness of this residue, the presence of the blue area is conditioned by the same cause indirectly through the preference for the methyl group over groups with partial negative charge in the 6-position. The red region near the 4- and 5-positions is formed by Q686 and Q405, while the yellow area at the 3-position is formed by N520 and I691. Therefore, the molecular model is consistent with the receptor mapping derived from CoMFA analysis. Nevertheless, only a part of the active site was mapped using CoMFA. For example, the area near the 1- and 2-positions did not appear to be mapped, since substituents at these positions do not vary in the data set. In addition, there is one discrepancy between the CoMFA plots and the molecular model: the interlobular space is depicted in the CoMFA plot by a yellow contour indicating steric hindrance instead of free space. The yellow region on the CoMFA plot is attributed to the decreased activity of ligands carrying bulky substituents in 3-position; however, this decrease can be explained not by steric hindrance but by the unfavorable solvation of hydrophobic substituents in the interlobular space. These two facts illustrate an important drawback of ligand-based QSAR models: their results are too biased by the size, diversity, and quality of the ligand databases used to develop them. This confirms that support of the conclusions from CoMFA modeling with proper protein modeling is desirable whenever such modeling is possible.

Structure-Based Quantitative Binding Model. We have studied an alternative method of building a quantitative model on the basis of known receptor structure. All compounds used for developing the aforementioned CoMFA model were docked to the 3D molecular model of the glycine site open form using the Sybyl 6.6 DOCK module. The computed values of electrostatic (E_{el}) and steric (E_{st}) interaction energy were used as descriptors for correlating with IC_{50} (Table 1). The resulting regression equation is

$$\log(^1/_{IC_{50}}) = -1.80 - 0.34E_{el} - 0.63E_s \qquad (1)$$

$$R = 0.838, \quad s = 0.66, \quad n = 88, \quad F = 100.5$$

where R is the multiple correlation coefficient, s is the standard error of estimate, n is the number of compounds, and F is the Fisher criterion. The scatter plot of observed vs predicted values of $\log(^1/_{IC_{50}})$ is shown in Figure 5. Although the statistical results of this model are somewhat worse in comparison with the abovementioned CoMFA model (0.838 vs 0.896 for the mul-

tiple correlation coefficient), this model in principle can be used for designing ligands belonging to different classes.

It should also be mentioned that the choice of descriptors in eq 1 is not arbitrary. There exists some analogy between eq 1 and the main equation of the linear interaction energy (LIE) approach to computing the free energy of ligand−protein binding.[33] Although the latter involves averaging over a molecular dynamics trajectory (instead of one-point calculation) and a separate simulation of a free ligand in solution, the functional form including weighted contributions of van der Waals and electrostatic ligand−protein interaction energies is common for both approaches. To extend the analogy, we have tried to include in the model descriptors accounting for interactions between ligands and the water solvent: free energy of solvation (computed with AMSOL[34]); polar and nonpolar surface areas (computed with PCMODEL[35]). However, the stepwise procedure of regression model construction has excluded the latter descriptors from the model as being statistically insignificant. Therefore, eq 1 appeared to be optimal for this kind of analysis.

Conclusion

Homology modeling and molecular dynamics simulations have been applied to building three-dimensional models of the NMDA receptor glycine binding site. These models were used to rationalize (1) distinctions between its agonists and antagonists, (2) known qualitative structure−activity relationships for its ligands, and (3) pharmacophore models for antagonists. In addition to the qualitative analysis, two quantitative models have been developed for antagonists. The first one was based on the CoMFA methodology, while the second one was based on the structure of a model of the glycine site and involved the use of docking energies for a quantitative description of ligand−protein interactions. The CoMFA model demonstrated slightly better correlation with potency than the docking energy model. Both models have successfully been applied to explain the binding affinities of NMDA receptor glycine site antagonists. These results provide tools for predicting the affinity of new glycine-site ligands, as well as for guiding the design and synthesis of new ligands.

Acknowledgment. We thank Tripos GmbH (Münich, Germany) and V. N. Orekhovich Institute of Biomedical Chemistry of Russian Academy of Medical Sciences for scientific and technical assistance. We acknowledge the University of California, San Francisco, for providing Amber 6.

References

(1) Wickelgren, I. Key brain receptor gets an unusual regulator. *Science* **1999**, *286*, 1265−1266.

(2) Parsons, C. G.; Danysz, W.; Quack, G. Glutamate in CNS Disorders as a Target for Drug Development: An Update. *Drug News Perspect.* **1998**, *11*, 523−579.

(3) Nakanishi, N. S. Molecular diversity of glutamate receptors and implications for brain function. *Science* **1992**, *258*, 31−37.

(4) (a) Tikhonova, I. G.; Baskin, I. I.; Palyulin, V. A.; Zefirov, N. S. Computer-assisted modeling of 3D structure of the NMDA receptor NR2B subunit glutamate site. *Dokl. Akad. Nauk* **2002**, *382*, 550−553. (*Dokl. Biochem. Biophys. (Transl. of Dokl. Akad. Nauk)* **2002**, *382* (4), 38−41). (b) Tikhonova, I. G.; Baskin, I. I.; Palyulin, V. A.; Zefirov, N. S.; Bachurin, S. O. Structural Basis for Understanding Structure−Activity Relationships for the Glutamate Binding Site of NMDA Receptor. *J. Med. Chem.* **2002**, *45*, 3836−3843, 5608. (c) For preliminary short communication, see the following. Tikhonova, I. G.; Baskin, I. I.; Palyulin, V. A.; Zefirov, N. S. A Spatial model of the glycine site of the NR1 subunit of NMDA receptor and ligand docking. *Dokl. Akad. Nauk* **2002**, *382*, 840−843. (*Dokl. Biochem. Biophys. (Transl. of Dokl. Akad. Nauk)* **2002**, *382* (6), 67−70).

(5) The model of the NMDA receptor ion channel was discussed earlier. Bachurin, S.; Tkachenko, S.; Baskin, I.; Lermontova, N.; Mukhina, T.; Petrova, L.; Ustinov, A.; Proshin, A.; Grigoriev, V.; Lukoyanov, N.; Palyulin, V.; Zefirov, N. Neuroprotective and Cognition-Enhancing Properties of MK-801 Flexible Analogs. Structure−Activity Relationships. *Ann. N. Y. Acad. Sci.* **2001**, *939*, 219−236.

(6) (a) Danysz, W.; Parsons, A. C. Glycine and *N*-methyl-D-aspartate receptors: physiological significance and possible therapeutic applications. *Pharmacol. Rev.* **1998**, *50*, 597−664. (b) Rowley, M.; Kulagowski, J. J.; Watt, A. P.; Rathbone, D.; Stevenson, G. I.; Carling, R. W.; Baker, R.; Marshall, G. R.; Kemp, J. A.; Foster, A. C.; Grimwood, S.; Hargreaves, R.; Hurley, C.; Saywell, K. L.; Tricklebank, M. D.; Leeson, P. D. Effect of plasma protein binding on in vivo activity and brain penetration of glycine/NMDA receptor antagonists. *J. Med. Chem.* **1997**, *40*, 4053−4068. (c) Kreimeyer, A.; Laube, B.; Sturgess, M.; Goeldner, M.; Foucaud, B. Evaluation and biological properties of reactive ligands for the mapping of the glycine site on the *N*-methyl-D-aspartate (NMDA) receptor. *J. Med. Chem.* **1999**, *42*, 4394−4404. (d) Jimonet, P.; Ribeill, Y.; Bohme, G. A.; Boireau, A.; Cheve, M.; Damour, D.; Doble, A.; Genevois-Borella, A.; Herman, F.; Imperato, A.; Le Guern, S.; Manfre, F.; Pratt, J.; Randle, J. C.; Stutzmann, J. M.; Mignani, S. Indeno[1,2-*b*]pyrazin-2,3-diones: a new class of antagonists at the glycine site of the NMDA receptor with potent in vivo activity. *J. Med. Chem.* **2000**, *43*, 2371−2381. (e) Cordi, A. A.; Desos, P.; Randle, J. C.;Lepagnol, J. Structure−activity relationships in a series of 3-sulfonylamino-2-(1H)-quinolones, as new AMPA/kainate and glycine antagonists. *Bioorg. Med. Chem.* **1995**, *3*, 129−141.

(7) Cai, S. X.; Zhou, Z. L.; Huang, J. C.; Whittemore, E. R.; Egbuwoku, Z. O.; Lu, Y.; Hawkinson, J. E.; Woodward, R. M.; Weber, E.; Keana, J. F. Synthesis and structure−activity relationships of 1,2,3,4-tetrahydroquinoline-2,3,4-trione 3-oximes: novel and highly potent antagonists for NMDA receptor glycine site. *J. Med. Chem.* **1996**, *39*, 3248−3255.

(8) Di Fabio, R.; Capelli, A. M.; Conti, N.; Cugola, A.; Donati, D.; Feriani, A.; Gastaldi, P.; Gaviraghi, G.; Hewkin, C. T.; Micheli, F.; Missio, A.; Mugnaini, M.; Pecunioso, A.; Quaglia, A. M.; Ratti, E.; Rossi, L.; Tedesco, G.; Trist, D. G.; Reggiani, A. Substituted indole-2-carboxylates as in vivo potent antagonists acting as the strychnine-insensitive glycine binding site. *J. Med. Chem.* **1997**, *40*, 841−850.

(9) Leeson, P. D.; Baker, R.; Carling, R. W.; Curtis, N. R.; Moore, K. W.; Williams, B. J.; Foster, A. C.; Donald, A. E.; Kemp, J. A.; Marshall, G. R. Kynurenic acid derivatives. Structure−activity relationships for excitatory amino acid antagonism and identification of potent and selective antagonists at the glycine site on the *N*-methyl-d-aspartate receptor. *J. Med. Chem.* **1991**, *34*, 1243−1252.

(10) Leeson, P. D.; Carling, R. W.; Moore, K. W.; Moseley, A. M.; Smith, J. D.; Stevenson, G.; Chan, T.; Baker, R.; Foster, A. C.; Grimwood, S. 4-Amido-2-carboxytetrahydroquinolines. Structure−activity relationships for antagonism at the glycine site of the NMDA receptor. *J. Med. Chem.* **1992**, *35*, 1954−1968.

(11) Cai, S. X.; Kher, S. M.; Zhou, Z. L.; Ilyin, V.; Espitia, S. A.; Tran, M.; Hawkinson, J. E.; Woodward, R. M.; Weber, E.; Keana, J. F. Structure−activity relationships of alkyl- and alkoxy-substituted 1,4-dihydroquinoxaline-2,3-diones: potent and systemically active antagonists for the glycine site of the NMDA receptor. *J. Med. Chem.* **1997**, *40*, 730−738.

(12) Cai, S. X.; Zhou, Z. L.; Huang, J. C.; Whittemore, E. R.; Egbuwoku, Z. O.; Hawkinson, J. E.; Woodward, R. M.; Weber, E.; Keana, J. F. Structure−activity relationships of 4-hydroxy-3-nitroquinolin-2(1H)-ones as novel antagonists at the glycine site of *N*-methyl-D-aspartate receptors. *J. Med. Chem.* **1996**, *39*, 4682−4686.

(13) Zhou, Z. L.; Navratil, J. M.; Cai, S. X.; Whittemore, E. R.; Espitia, S. A.; Hawkinson, J. E.; Tran, M.; Woodward, R. M.; Weber, E.; Keana, J. F. Synthesis and SAR of 5-, 6-, 7- and 8-aza analogues of 3-aryl-4-hydroxyquinolin-2(1H)-one as NMDA/glycine site antagonists. *Bioorg. Med. Chem.* **2001**, *9*, 2061−2071.

(14) Kuryatov, A.; Laube, B.; Betz, H.; Kuhse, J. Mutational analysis of the glycine-binding site of the NMDA receptor: structural similarity with bacterial amino acid-binding proteins. *Neuron* **1994**, *12*, 1291−1300.

(15) Armstrong, N.; Gouaux, E. Mechanisms for activation and antagonism of an AMPA-sensitive glutamate receptor: crystal structures of the GluR2 ligand binding core. *Neuron* **2000**, *28*, 165−181.

(16) Cramer, R. D., III; Patterson, D. E.; Bunce, J. D. Comparative molecular field analysis (CoMFA). 1. Effect of shape on binding of steroids to carrier proteins. *J. Am. Chem. Soc.* **1988**, *110*, 5959−5967.
(17) Bairoch, A.; Apweiler, R. The SWISS−PROT protein sequence database and its supplement TrEMBL in 2000. *Nucleic Acids Res.* **2000**, *28*, 45−48.
(18) Thompson, J. D.; Gibson, T. J.; Plewniak, F.; Jeanmougin, F.; Higgins, D. G. The CLUSTAL X windows interface: flexible strategies for multiple sequence alignment aided by quality analysis tools. *Nucleic Acids Res.* **1997**, *25* (24), 4876−4882.
(19) *Sybyl 6.6*; Tripos Associates: St. Louis, MO, 1999.
(20) Case, D. A.; Pearlman, D. A.; Caldwell, J. W.; Cheatham, T. E., III; Ross, W. S.; Simmerling, C. L.; Darden, T. A.; Merz, K. M.; Stanton, R. V.; Cheng, A. L.; Vincent, J. J.; Crowley, M.; Tsui, V.; Radme, R. J.; Duan, Y.; Pitera, J.; Massova, I.; Seibel, G. L.; Singh, U. C.; Weiner, P. K.; Kollman, P. A. *AMBER 6*; University of California, San Francisco, 1999.
(21) Cornell, W. D.; Cieplak, P.; Bayly, C. I.; Gould, I. R.; Merz, K. M., Jr.; Ferguson, D. M.; Spellmeyer, D. C.; Fox, T.; Caldwell, J. W.; Kollman, P. A. A second generation force field for the simulation of proteins, nucleic acids, and organic molecules. *J. Am. Chem. Soc.* **1995**, *117*, 5179−5197.
(22) Lüthy, R.; Bowie, J. U.; Eisenberg, D. Assessment of protein models with three dimensional profiles. *Nature* **1992**, *356*, 83−85.
(23) Laskowski, R. A.; MacArthur, M. W.; Moss, D. S.; Thornton, J. M. PROCHECK: A program to check the stereochemical quality of protein structures. *J. Appl. Crystallogr.* **1993**, *26*, 283−291.
(24) Rullmann, J. A. C. *AQUA*; Utrecht University: Utrecht, The Netherlands, 1996.
(25) Bayly, C. I.; Cieplak, P.; Cornell, W. D.; Kollman, P. A. A Well-Behaved Electrostatic Potential Based Method Using Charge Restraints for Determining Atom-Centered Charges: The RESP Model. *J. Phys. Chem.* **1993**, *97*, 10269−10280.
(26) Colquhoun, D. Binding, gating, affinity, and efficacy: The interpretation of structure−activity relationships for agonists and of the effects of mutating receptors. *Br. J. Pharmacol.* **1998**, *125*, 924−947.
(27) Leeson, P. D.; Carling, R. W.; Smith, J. D.; Baker, R.; Foster, A. C.; Kemp, J. A. *trans*-2-Carboxy 4-substituted tetrahydroquinolines: Potent glycine-site NMDA receptor antagonists. *Med. Chem. Res.* **1991**, *1*, 64−73.
(28) Kessler, M.; Baudry, M.; Lynch, G. Quinoxaline derivatives are high-affinity antagonists of the NMDA receptor glycine sites. *Brain Res.* **1989**, *489*, 377−382.
(29) Sheardown, M. J.; Drejer, J.; Jensen, L. H.; Stidsen, C. E.; Honore, T. A potent antagonist of the strychnine insensitive glycine receptor has anticonvulsant properties. *Eur. J. Pharmacol.* **1989**, *174*, 197−204.
(30) Verdoorn, T. A.; Kleckner, N. W.; Dingledine, R. *N*-Methyl-D-aspartate/glycine and quisqualate/kainate receptors expressed in xenopus oocytes: Antagonist pharmacology. *Mol. Pharmacol.* **1989**, *35*, 360−368.
(31) Nikam, S. S.; Cordon, J. J.; Ortwine, D. F.; Heimbach, T. H.; Blackburn, A. C.; Vartanian, M. G.; Nelson, C. B.; Schwarz, R. D.; Boxer, P. A.; Rafferty, M. F. Design and synthesis of novel quinoxaline-2,3-dione AMPA/GlyN receptor antagonists: amino acid derivatives. *J. Med. Chem.* **1999**, *42*, 2266−2271.
(32) Morris, G. M.; Goodsell, D. S.; Halliday, R. S.; Huey, R.; Hart, W. E.; Belew, R. K.; Olson, A. J. Automated Docking Using a Lamarckian Genetic Algorithm and Empirical Binding Free Energy Function. *J. Comput. Chem.* **1998**, *19*, 1639−1662.
(33) Åqvist, J.; Medina, C.; Samuelsson, J. E. A new method for predicting binding affinity in computer-aided drug design. *Protein Eng.* **1994**, *7*, 385−391.
(34) Hawkins, G. D.; Giesen, D. J.; Lynch, G. C.; Chambers, C. C.; Rossi, I.; Storer, J. W.; Li, P.; Winget, D.; Renaldi, D.; Liotard, D. A.; Cramer, C. J.; Truhlar, D. G. *AMSOL*, version 6.7.2; University of Minnesota: Minneapolis, MN, 2001 (based in part on AMPAC, version 2.1, by Liotard, A. D.; Healy, E. F.; Ruiz, J. M.; Dewar, M. J. S).
(35) Serena Software, Box 3076, Bloomington, IN 47402-3076.

JM0210156